Journal of Applied Polymer Science

Crystallization and Thermal Properties of Polylactide/Palygorskite Composites

Sreejarani Kesavan Pillai,[1] Vincent Ojijo,[1] Suprakas Sinha Ray[1,2,3]

[1]DST/CSIR Nanotechnology Innovation Centre, National Centre for Nano-Structured Materials, Council for Scientific and Industrial Research, Pretoria 0001, South Africa

[2]Department of Applied Chemistry, University of Johannesburg, Doornfontein 2028, Johannesburg, South Africa

[3]Department of Chemistry, King Abdulaziz University, Jeddah 21589, Kingdom of Saudi Arab

Correspondence to: S. K. Pillai (E-mail: skpillai@csir.co.za)

ABSTRACT: Polylactide palygorskite (fibrous clay) composites were prepared by solvent casting method. Both pristine and organically modified palygorskite were used for composite preparation. The detailed crystallization behavior, morphology, and thermal properties of neat polylactide and the corresponding composites were investigated by using differential scanning calorimetry, polarized optical microscopy, scanning electron microscopy and wide angle X-ray diffraction techniques. The results showed that the crystallization and thermal characteristics of neat PLA were influenced significantly by the presence of palygorskite nanoparticles. © 2014 Wiley Periodicals, Inc. J. Appl. Polym. Sci. **2014**, *131*, 40414.

KEYWORDS: composites; crystallization; thermal properties; paly

Received 28 August 2013; accepted 9 January 2014
DOI: 10.1002/app.40414

INTRODUCTION

The biodegradable and biocompatible polymers have caused significant attention from both ecological and biomedical perspectives in the past decade.[1] Because polylactide (PLA), which is made from renewable resources has attractive features such as sustainability, biocompatibility, and biodegradability as well as physical properties comparable to petroleum-based polyolefins, it is considered as one of the most promising polyesters for various end-use applications.[2] However, the main drawback of PLA is its slow crystallization kinetics which limits the processability of the polymer.[3] This specifically becomes an issue when PLA is to be used in extrusion and injection moulding where it is hard to get high PLA crystallinity in a short time.[4] Therefore, how to enhance crystallization kinetics and increase crystallinity of PLA has been of great research interest in polymer processing field. Incorporation of additives such as plasticizers (e.g., triethyl citrate, polyethylene glycol) and nucleating agents (nanoclays, natural fibers, and inorganic compounds) have been recently considered as good strategies to obtain higher crystallinity and faster crystallization of PLA.[5] Among these additives, nanometer sized clay platelets (layerd silicates) are popular as it is well established that when dispersed properly, they can act as effective nucleation sites enhancing the crystallization rate of PLA matrix.[6] Moreover, the large aspect ratio of the silicate layers results in a high interfacial area minimizes the chain mobility, and creates a reinforcement effect, thus leads to concurrent improvement of other properties of the polymer.[7]

Several articles report on the method to disperse clay particles into PLA matrix, to get improvement in properties. Two main techniques are used to obtain nanodispersion of clay particles in PLA matrix namely the solution-intercalation[8,9] and the melt-blending processes.[10–13] The dispersion of hydrophilic clay mineral particles in hydrophobic polymer matrix often poses problems in the development of composite materials which ultimately affect their properties. Generally, organic modification of the clay particles is done to improve the interaction between the PLA chains and clay platelets. The organic modification thus leads to improved dispersion of clay particles in the PLA matrix as opposed to the raw clay without organic modification.[8,10–14] *In situ* polymerizations, where the growing polymer chains are grafted on the clay surface is another way to obtain a good dispersion of clay in a PLA matrix.[15]

Capability of layered silicates (nanoclays) in influencing the crystallization rate and properties of PLA has been demonstrated by many research groups. Ray et al.[16–18] studied the detailed isothermal crystallization behavior and kinetics of clay-containing nanocomposites of PLA. They observed that the clay

Additional Supporting Information may be found in the online version of this article.

particles act as a nucleating agent for PLA crystallization and increases the overall crystallization rate remarkably while not influencing the linear growth of the polymer. Incorporation of organically modified montmorillonite (OMMT) improved the material properties such as dynamic mechanical properties both in solid and melt state, flexural properties, gas permeability, and biodegradability when compared to neat PLA. Similar nucleation effect of MMT clay and PLA property enhancement has also been reported by Pluta et al.[14] Lee and Jeong[19] recently showed that the overall melt-crystallization rates of PLA increased considerably by the addition of only ~3 wt % polyhedral oligomeric silsesquioxane-modified MMT (POSS-MMT), indicating that the clay nanoparticles served as acceleration agents for the overall melt-crystallization of PLA. Paul et al.[10] observed an increase in thermal stability of PLA matrix when filled with 3 wt % of OMMT (C30B) along with PEG (polyethylene glycol). McLauchlin et al. also[20] reported improved thermal properties of PLA composites containing 4 wt% of cocamidopropylbetain modified MMT.

Most of the literature regarding composites of PLA and their property enhancement is devoted to lamellar layered silicates, in particular MMT and OMMT due to their ability to significantly enhance several polymer physical properties as compared to unmodified layered silicate clays. However, reports on PLA composites with clay particles with different morphologies are scarce.

Palygorskite (Paly) is a fibrous silicate (diameter 10–25 nm, length: 1000 nm) with needle like morphology having chemical formula of $(Mg, Al)_5Si_8O_{20}(OH)_2(OH_2)_4(H_2O)_4$.[21] The high aspect ratio, surface area and fibrous structure make it an chemical formula as reinforcing nanofillers in various polymer matrices. Recently, Paly based composites are gaining a lot of research interest. Yin et al.[22] studied the rheological properties of polyacrylonite containing Paly in melt state and found that the mechanical property improvement of the matrix is much more significant at high temperature than that at lower one. Sun et al.[23] reported enhanced tensile properties of polytetraflouroethylene fabric composites prepared using silane treated Paly. Shen et al.[24] showed that the incorporation of the Paly causes the polymer network to exhibit reinforcement in thermal and mechanical properties and slower relaxation in segment mobility compared to neat polyamides. Peng et al.[25] homogeneously dispersed isaophrone diisocyanate modified Paly in the waterborne polyurethane which resulted in an improvement of thermal stability, tensile strength and elongation at break of the composites. Chen[26] reported the nucleation effect of Paly in poly (butylene succinate) composite. However, so far to our knowledge, the influence of Paly in matrix modification of PLA has hardly been studied.

The aim of this work was to study the effect of the addition of pristine and organically modified Paly on the crystallization, thermal properties and morphology of neat PLA. The composites were prepared by solvent casting method. The detailed crystallization kinetics and morphology of neat PLA and the corresponding composites were investigated by using differential scanning calorimetry (DSC), polarized optical microscopy (POM), scanning electron microscopy (SEM) and wide angle X-ray diffraction techniques (XRD) and Fourier transform infrared spectroscopy (FTIR).

EXPERIMENTAL

Materials

The PLA used in this study was a commercial grade (PLA 2002D), obtained from the Natureworks, LLC (USA). It had a D-isomer content ~4 wt %; weight average molecular weight, $M_w = 235$ kg mol^{-1}; density = 1.24 g cm^{-3}; glass transition temperature, $T_g =$ ~53°C; and melting temperature, $T_m = 153$°C. The raw Paly was obtained from Sud Chemie, South Africa. Organically modified Paly (Org-Paly) was prepared in house by cation exchange reaction between pristine clay with a quaternary ammonium salt di (hydrogenated tallow) dimethyl ammonium chloride (Arquad 2HT-75). Reagents such as chloroform, ethanol and Arquad 2HT-75, were purchased from Sigma Aldrich and used as received without further purification.

Methods

Organic Modification of Paly. In a typical procedure, 2 g of Paly was dispersed in 200 mL deionized water and magnetically stirred for 30 min. A calculated amount of surfactant (equal to the cation exchange capacity (CEC) of the clay = 35 meq/100 g) was dissolved in minimum amount of ethanol and added dropwise to the clay suspension. The mixture was then magnetically stirred for 24 h at 60°C. The solution was filtered, washed several times with de-ionized water and oven dried at 50°C overnight. The dried sample was ground to get uniform particle size. The sample was designated as Org-Paly X, where X represents the wt % of Org-Paly. The organic content in Org-Paly measured by TGA was 12 wt % (this corresponds to the % weight loss due to surfactant decomposition in the temperature range 250–350°C, please refer Supporting Information for TGA results).

Preparation of Composite Films. PLA composites with 1–5 wt % filler content (Paly and Org-Paly) were prepared by solvent-casting method. 10 g of PLA was dissolved in 100 mL $CHCl_3$ by ultrasonication (Bondelin Sonex Ultrasonicator, 35 kHz, 80W, exposure time 20 min). Required amount of clay was added to the polymer solutions and magnetically stirred for 2 h at room temperature. The mixture was then poured into Petri dishes and the solvent was allowed to evaporate. The films were peeled off the next day and annealed at 80°C overnight. Neat PLA film was also prepared under the same conditions for comparison.

Characterization of Powder Clay Samples. The size and shape of clay particles were analyzed by a JEOL 2100 TEM, operated at 200 kV. The TEM samples were prepared by sonicating clay powder in methanol for 5 min, followed by depositing the solution on a carbon coated Cu-grid. The surface morphology of the powder samples were analyzed using a JEOL 7500 FE SEM. The FTIR spectra of raw and modified clays were recorded by a Perkin-Elmer spectrum 100 FTIR spectrometer. The XRD analyses were performed with a PANalytical X'PERT-PRO diffractometer using Ni filtered Cu Kα radiation (wave length, $\lambda = 1.5406$

Å) with a fixed slit at 45 kV and 40 mA in the angle range of $2° < 2\theta < 80°$.

Characterization of Composite Films. The thermal properties of neat PLA and various PLA/Paly composites were performed by means of a DSC Q2000 instrument (TA Instruments) in nitrogen atmosphere at a flow rate of 50 mL min^{-1}. The samples (4–7 mg) were sealed in aluminum pans. Samples were first equilibrated at −25°C, then to 200°C at a rate of 20°C min^{-1}, kept at this temperature for 5 min to erase previous thermal history, cooled down to −25°C at 20°C min^{-1}, and then repeated heating scan from −25 to 200°C at a rate of 5°C min^{-1}. The cold crystallization peak (T_{cc}), melting peak (T_m) temperatures, and the degree of crystallization (χ_c) of PLA matrix were determined from the thermograms. χ_c was calculated according to the relation $\chi_c = [\Delta H_m/\omega\Delta H_f] \times 100$, where ω is the weight fraction of PLA component, ΔH_m is the enthalpy of melting and ΔH_f is the heat of fusion of 100% crystalline PLA (taken as 93 J g^{-1}).[16] A FESEM (JEOL 7500 FE SEM) was used to characterize the surface morphology of the fractured surface of the PLA and composite films. The XRD analyses were performed with a PANalytical X'PERT-PRO diffractometer using Ni filtered CuKα radiation ($\lambda = 1.5406$ Å) with a fixed slit at 45 kV and 40 mA in the angle range of $2° < 2\theta < 80°$ (step size = 0.0262606 deg, time / step = 181.05 s, scan speed = 0.036987 deg s^{-1}). The composite film samples were mounted on a metallic sample holder with sticky tape. The effect of incorporation of clay particles on the spherulitic growth behavior of PLA matrix was studied using POM. The thin sample was prepared by pressing the film between two cover glasses using a Linkam hot stage. The samples were then melted at 200°C and cooled to 120°C at 10°C min^{-1}. They were then held isothermally at 120°C and crystallized for desired time during which images were taken by a Carl Zeiss polarized optical microscope. ^{1}H NMR analyses were done using an Agilent Variance 600 MHz spectrometer with $CDCl_3$ as solvent and tetramethylsilane as internal standard.

RESULTS AND DISCUSSION

Characterization of Powder Samples

FTIR spectroscopy was used to characterize the effectiveness of organic modification in Paly. Figure 1 shows the FTIR spectra of the unmodified and organically modified Paly which showed typical vibrational bands of aluminosilicates. In the high frequency range, peaks at 3633, 3381, and 1635 cm^{-1} are associated to the stretching mode of the OH-group coordinated to Al cations,[21,27] interlayered O—H stretching (H bonding) and H—O—H bending, respectively. In the low frequency region, the bands at 1098 and 1018 cm^{-1} are related to the stretching of Si—O—Si bond, characteristic of phyllosilicate minerals.[28] Mg—Al—OH and Al—Al—OH deformations are observed at 848 and 921 cm^{-1}; whereas the two strong bands at 667 and 550 cm^{-1} correspond to the bending mode of Si—O and Si—O—M bonds (where M = Mg, Al and Fe), respectively.[29] In the case of Org-Paly, additional peaks observed at 2924 and 2849 cm^{-1} are associated with the asymmetric and symmetric stretching vibrations of alkyl groups of the surfactant,[30] respectively, which indicates the successful organic modification of Paly. The

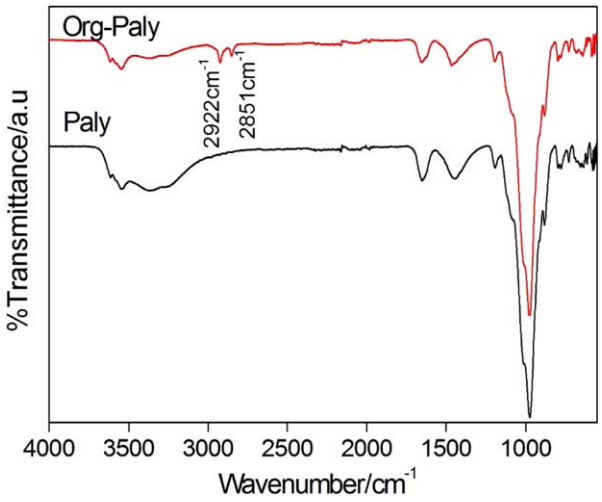

Figure 1. FTIR spectra of Paly and Org-Paly. [Color figure can be viewed in the online issue, which is available at wileyonlinelibrary.com.]

adsorption of the surfactant occurs through electrostatic attraction between the surface hydroxyl groups of Paly and ammonium group of Arquad 2HT-75.[31]

Parts (a, a') and (b, b') of Figure 2 presents the SEM and corresponding TEM micrographs of Paly and Org-Paly, respectively. In the SEM image, Paly appears as straight fibers that are oriented randomly and as aggregates of sheet-like layers of rods. The fibers are entangled to each other due to the strong interaction between the fibers. The morphological differences between Org-paly and Paly are not very distinct from the TEM images, but are evident from the SEM images. The surface of Paly appears to be clean and smooth unlike that of Org-Paly. The deposition of a polymer-like coating along the sidewalls of the fibers is visible for Org-Paly, which could be due to the possible adsorption of the surfactant on the outer surface. TEM images show that the degree of aggregation increases with organic modification.

The XRD patterns of Paly and Org-Paly are shown in Figure 3. Paly shows intense peaks at $2\theta = 8.5$, 20.8, and 26.5°, which correspond to the 110, 121, and 231 planes, respectively of orthorhombic crystals of paly (reference code: 00-021-0550).[32] No obvious differences on the XRD pattern is observed in the case of Org-Paly indicating that the modification with organic surfactant did not change the structure of Paly. This is due to the fact the Paly is a nonswelling clay and the adsorption of cationic surfactant is limited to the external surface because there is no interlayer space.[33] The surfactant molecules on fibrous clays usually are adsorbed in multi-layers, with the first layer formed by electrostatic attraction between surfactant and Paly surface, whereas the other layers are formed by hydrophobic bonds between surfactant molecules.[34] This result is in line with the SEM observations.

Characterization of Composite Films

The dispersion/distribution of Paly and Org-Paly particles in PLA matrix was studied with a FESEM. Parts (a) and (b) of Figure 4, respectively, show the tensile fractured-surface morphology of PLA/Paly (2 wt %) and PLA/Org-Paly (2 wt %)

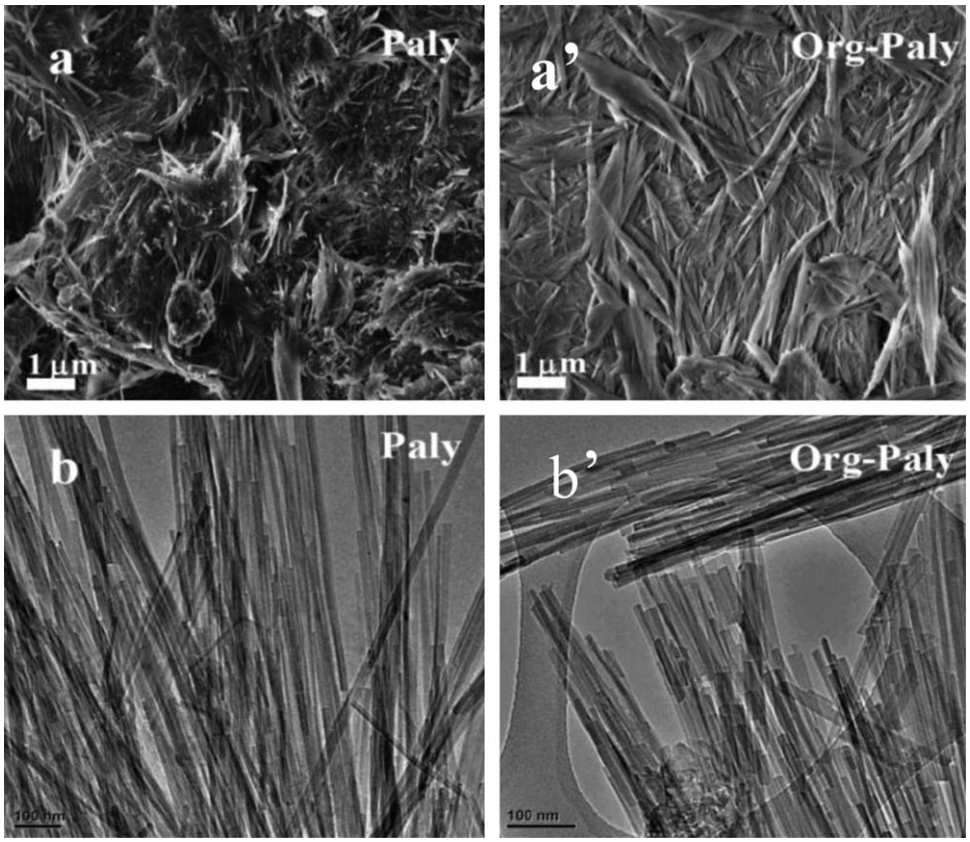

Figure 2. FESEM images of (a) Paly (a') Org-Paly and Bright field TEM images of (b) Paly (b') Org-Paly.

composite films. PLA loaded with 2 wt % Paly shows a reasonably good degree of dispersion when compared to the PLA/Org-Paly composite containing the same amount of organo clay loading. Paly nanoparticles show a tendency to aggregate in PLA matrix when the clay content is increased to 5 wt %. Higher degree of nanoparticle aggregation and interfacial debonding is observed in the case of composites containing Org-Paly (aggregation is observed from 2 wt % of Org-Paly) with pull-outs during fracture [refer to Figure 4(b)]. The presence of hydrophobic surfactant on Paly surface may result in weak interaction between the silanol (Si—OH) group of Paly and ester group of PLA which thus causes aggregation of Org-Paly.[31] Better interfacial bonding and more homogeneous dispersion of pristine Paly in PLA matrix probably is due to availability of free Si—OH groups to interact with PLA ester groups. This result is similar to that of Liu et al.[31] where they observed reduced thermal stability and compatibility of organically modified sepiolite in PLA matrix.

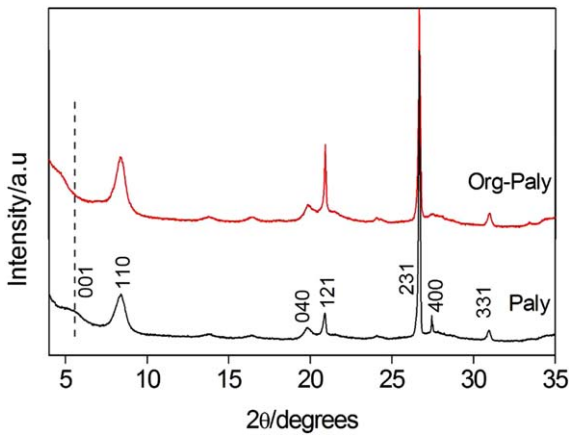

Figure 3. XRD spectra of Paly and of Org-Paly. [Color figure can be viewed in the online issue, which is available at wileyonlinelibrary.com.]

Figure 5(a) shows the second heating DSC thermograms of annealed neat PLA and PLA/Paly composite films. Figure 5(b) shows the corresponding DSC thermograms of neat PLA and PLA/Org-Paly composites, and the parameters determined from these DSC scans are summarized in Table I. Crystallization of PLA on cooling is negligible and is not affected by the incorporation of Paly or Org-Paly which is confirmed by the absence of exotherm in the cooling DSC curves (not given).[35] However, PLA crystallizes on heating and it is found that the crystalline phase melts with double-peak endotherm in the second heating curves of PLA/Paly whereas the melting occurred with a single peak in PLA/Org-Paly samples. The bimodal melting peaks in the case of Paly containing composites can be attributed to the formation of α (stable, melts at higher temperature) and β (less stable, melts at lower temperature) crystal structures of PLA due to faster crystallization process in presence of Paly.[36–38]

The T_g for all the samples is seen clearly which indicates that all the samples are constraint free after annealing at 80°C overnight. The incorporation of Paly increases the T_g of PLA

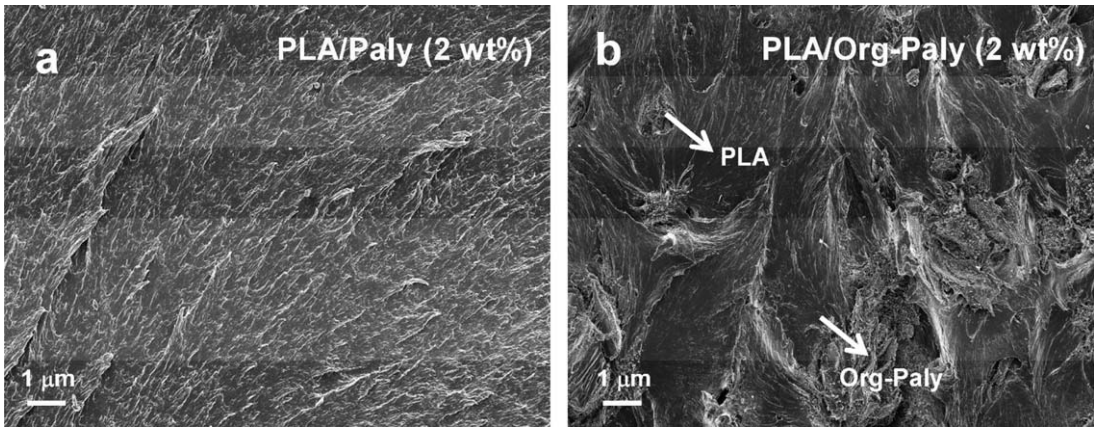

Figure 4. FESEM fractured-surface image of (a) PLA/Paly (2 wt %) and (b) PLA/Org-Paly (2 wt %) composite films.

significantly up to a Paly content of 2 wt %, which may be due to the good dispersion and interaction of clay particles in the polymer phase. A reduction in T_g is observed for the film containing 5 wt % of clay. This is attributed to the increase in polymer mobility[39] due to the aggregation of clay particles which is in line with the SEM observations. Fukushima et al.[35] also observed poor dispersion and aggregation of sepiolite in PLA matrix at 5 and 7 wt % loading.

The sharp cold-crystallization peak observed for PLA/Paly samples indicates that, the cold crystallization process of PLA matrix takes place from a single homogeneous phase. However, it is interesting to note that the cold crystallization peak temperature of neat PLA moves toward much lower temperatures in the case of composites, and it is significant in the case of PLA/Paly (2 wt.%) composite. This decrease in T_{cc} is an indication of faster crystallization of PLA under the influence of Paly nanoparticles. Sabzi et al.[40] recently reported similar results on PLA/sepiolite composites and found that sepiolite nanoparticles have higher nucleation effect than nano-sized $CaCO_3$. Remarkable increase in crystallinity is observed in all the composites containing Paly which is due to the homogeneous dispersion of Paly nanoparticles in the PLA matrix, which consequently act as nucleators of the PLA chains to fold and join the crystallization growth front efficiently.[41] Effect of sepiolite in promoting the crystallization of PLA by inducing higher order crystalline zones is also reported by Fukushima et al.[35]

For the composite films prepared using Org-Paly [refer to Figure 5(b)], the thermograms showed weak melting peaks with undefined cold crystallization peaks indicating weaker nucleating power of Org-Paly. The extent of T_g increase and degree of crystallization observed in this case is not as much as that of composites containing unmodified Paly which indicates that the interphase between PLA matrix and nanofillers is weak due to the lack of interaction with the more aggregated clay particles.[42] For composite containing 5 wt % Org-Paly, the T_g decreases significantly when compared to neat PLA (52–44°C). Since the adhesion of the surfactant on fibrous clay surface is not strong, the surfactant can dissociate from the clay particles easily and leach out to the polymer matrix. Hence the leaching or plasticization by the de-bonded surfactants which can interact with the

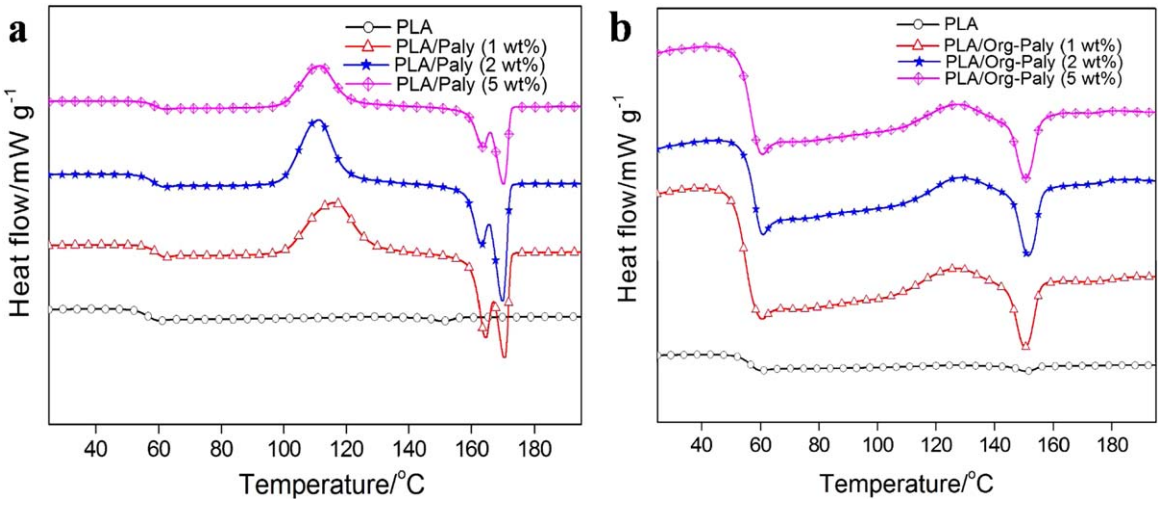

Figure 5. Second heating DSC thermograms (a) PLA and PLA/Paly composites (b) PLA and PLA/Org-Paly composites. [Color figure can be viewed in the online issue, which is available at wileyonlinelibrary.com.]

Table I. Thermal Properties of Neat PLA and Composites Calculated from DSC Thermograms

Films	T_g (°C)	T_{cc} (°C)	ΔH_m (J g^{-1})	χ_c (%)
PLA	52.6 ± 0.5	-	-	
PLA/Paly (1 wt %)	53.1 ± 0.5	116.5 ± 0.3	31.0 ± 1.0	33.3 ± 0.4
PLA/Paly (2 wt %)	57.2 ± 0.4	111.5 ± 0.6	33.0 ± 0.5	35.5 ± 0.9
PLA/Paly (5 wt %)	52.5 ± 0.4	111.1 ± 0.7	30.6 ± 0.9	32.9 ± 0.5
PLA/Org-Paly (1 wt %)	52.0 ± 0.9	-	1.7 ± 1.5	1.8 ± 1.0
PLA/Org-Paly (2 wt %)	55.4 ± 0.7	-	1.9 ± 0.5	2.0 ± 0.9
PLA/Org-Paly (5 wt %)	44.7 ± 0.6	-	2.2 ± 0.8	2.4 ± 1.0

PLA matrix could be a reason for this observation. Jalavandi et al.[43] also observed a reduction in T_g from 59 to 54°C for PLA containing 4 wt % MMT in presence of 28% starch and 12 wt % glycerol due to plasticizing effect.

The possibility of surfactant leaching in PLA matrix from org-paly was investigated by ^{1}H NMR analyses. Figure 6(a,b) show ^{1}H NMR spectra of the neat PLA and that of PLA/Org-Paly composite samples respectively. Any change in the chemical environment of the protons through chemical interactions is generally reflected by the disappearance of existing peaks, appearance of new set of peaks or a chemical shift. It is noteworthy that the split signals corresponding to methylene of the terminal groups (CH_2—OH) of neat PLA appearing at $\delta = 3.719$, 3.708 ppm,[44,45] are not seen in the composite. This indicates the interaction of Org-Paly with the PLA matrix. Although the results of NMR cannot give very specific information, it still confirms the occurrence of some sort of chemical interaction between the Org-Paly and PLA.

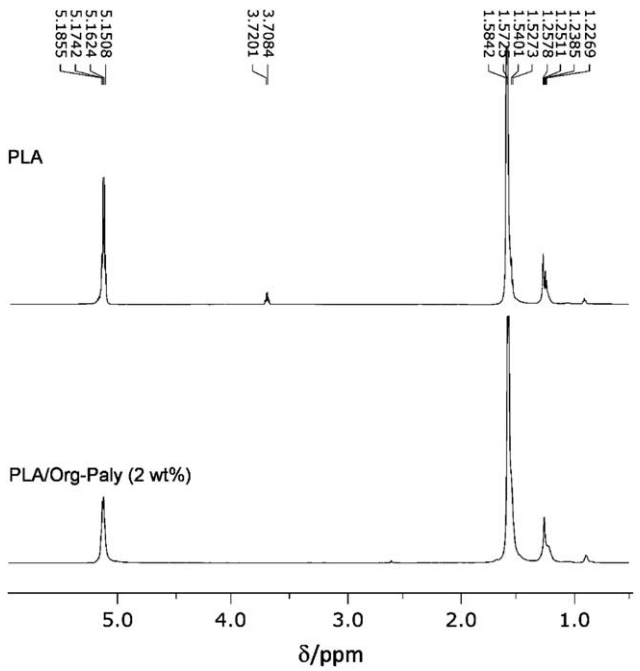

Figure 6. ^{1}H NMR spectra of (a) neat PLA and (b) PLA/Org-Paly (2 wt %) composites.

To confirm the nucleation effect of Paly on the enhanced melt-crystallization rates of the composites, the spherulite evolution during the melt-crystallization at 120°C for the neat PLA and the composites was monitored as a function of time and the observations are shown in Figure 7. From the time-dependent POM image of neat PLA, it is clear that the nucleation starts much later indicating higher activation energy for nucleation process. On the other hand, the nucleation density in composites containing Paly is much higher and the crystallization is completed much faster. It supports the fact that the clay nanoparticles dispersed in the composites serves as nucleating agents for PLA crystals during the isothermal crystallization. For the film containing Org-Paly, the spherulite formation is found to be very slow. Though the composites with 2 and 5 wt % of Org-Paly shows higher nucleation densities in comparison to the neat PLA, the results indicate that raw Paly has higher efficiency as nucleating agents. Although organic modification reduced the aggregation of clay particles in general in the case of Paly, presence of surfactant molecules on the external surface found to increase the clustering. The smaller surface area of such aggregated clay particles therefore does not facilitate the nucleation process of PLA crystals in comparison to the smaller particles of raw Paly. These observations are in agreement with the DSC results. These results are comparable to the highly enhanced overall melt crystallization of PLA in presence of POSS-modified MMT reported by Lee and Jeong.[19] Rapid completion of overall crystallization due to increased nucleation density in PLA by incorporating modified carbon black as efficient nucleating agents are recently reported by Su et al.[46] also.

The XRD patterns of neat PLA and the composites are shown in Figure 8. It can be seen that the characteristic diffraction peaks of PLA appears at $2\theta = 16.78$. This peak is assigned to the reflection of α-phase crystallite of PLA, which is orthorhombic with chains in a −10/3 helical conformation.[47] PLA peak positions remain unchanged in the composites indicating that the crystal structure of PLA is not altered by the presence of nanofillers. The characteristic XRD Peaks of Paly becomes prominent only at high loadings (2 and 5 wt %) as revealed by the reflections at $2\theta = 8.5$ and 20.8.[32] The decrease in intensity of α-peak of PLA in PLA/Paly composites could be due to the concurrent formation defective β crystal structures of PLA owing to faster crystallization process in presence of Paly.[36–38] This observation is in agreement with DSC and POM results. Being a non-

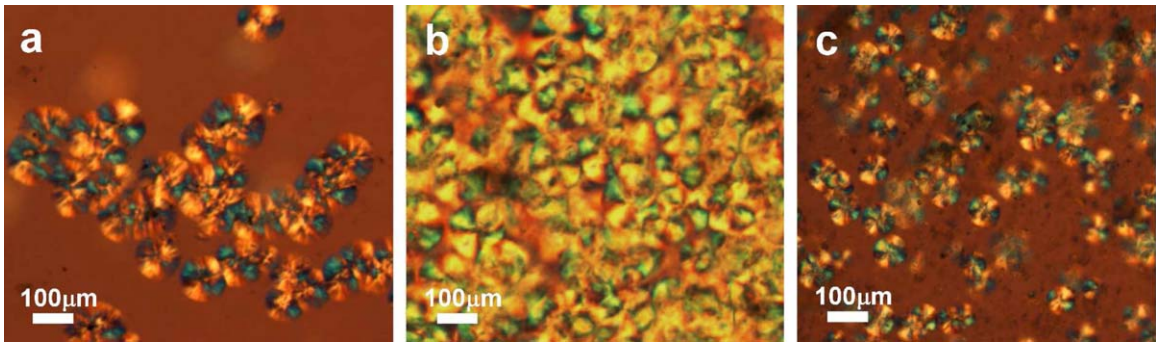

Figure 7. POM images taken during isothermal melt crystallization (a) neat PLA (at 45 min) (b) PLA/Paly (2 wt %) (at 24 min), and (c) PLA/Org-Paly (at 45 min). [Color figure can be viewed in the online issue, which is available at wileyonlinelibrary.com.]

swelling clay mineral, the dispersion of Paly cannot be understood from XRD results.[35]

To gain insight into possible structural changes induced by the incorporation of fillers, FT-IR spectra of the neat polymer and composites were recorded in the range of 550–4000 cm^{-1} (refer Figure 9). Although the peak positions for PLA remain unaltered PLA/Paly in the composites, the characteristic absorption peak corresponding to the bending mode of hydroxyl groups[48] in Paly (seen at 1750 cm^{-1}) is almost disappeared in PLA/Org-Paly composites. This result shows that there is less availability of the surface hydroxyl groups due to the modification of Paly surface by organic surfactant. The carbonyl group appearing at 1642 cm^{-1} for neat PLA shifts slightly toward higher wavenumber (1646 cm^{-1}) in PLA/Org-Paly composites indicating some degree of chemical interaction between Org-Paly and PLA matrix. Although org-paly is aggregated in PLA matrix, interaction is possible between the relatively smaller amount of surfactant groups left on the aggregate surface and PLA matrix. This is also confirmed by the ^1H NMR results. However, we believe that the aggregation of organically modified clay particles outweighs the interaction effect and hence the expected improvement in nucleation and thermal properties in the corresponding composites is not achieved.

Fukushima et al.[49] prepared PLA composite by adding 5 wt % of a sepiolite and obtained significant level of PLA degradation in compost at 58°C by a preferential mechanism of bulk degradation. In another study, they also found that biopolymer composites containing sepiolite exhibit improvement in thermomechanical properties as well as noncytotoxicity according biocompatibility tests with human cells.[35] Although addition of palygorskite could represent a real opportunity to obtain similar ecocompatible materials with high potential for industrial applicability, the influence of these nanoparticles on the polymer biodegradation and biocompatibility are to be investigated in detail.

CONCLUSIONS

PLA composites containing clay nanoparticles of fibrous morphology (Paly) were prepared by solvent casting technique. The degree of dispersion of both pristine and organically modified Paly in PLA matrix was studied in detail and correlated to the crystallization behavior, morphology and thermal properties of composites. The SEM results showed that the organic modification increased the aggregation tendency of Paly in PLA matrix in comparison to raw clay which could be attributed to the presence of less stable surfactant molecules adsorbed on clay

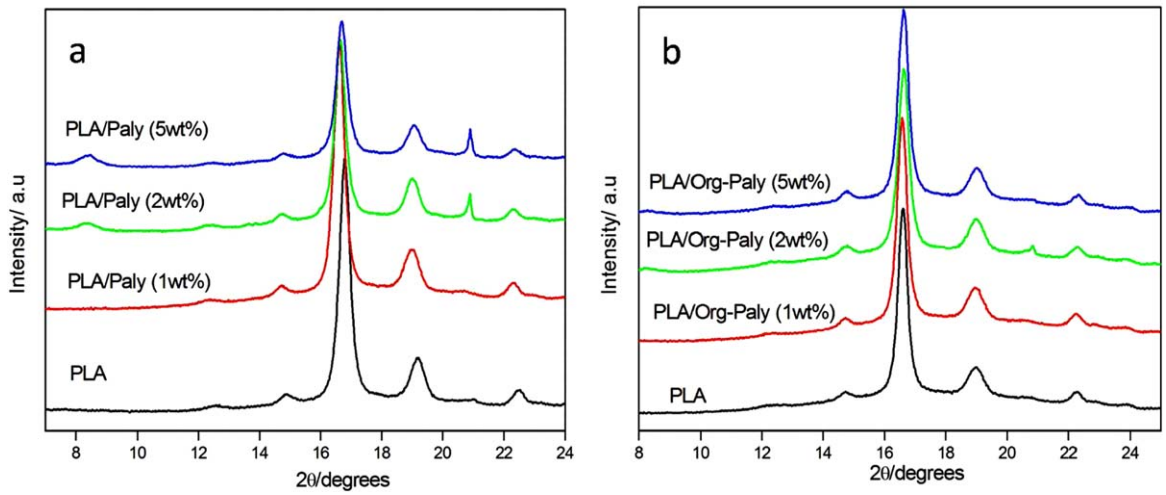

Figure 8. XRD patterns of (a) PLA and PLA/Paly composites (b) PLA and PLA/Org-Paly composites. [Color figure can be viewed in the online issue, which is available at wileyonlinelibrary.com.]

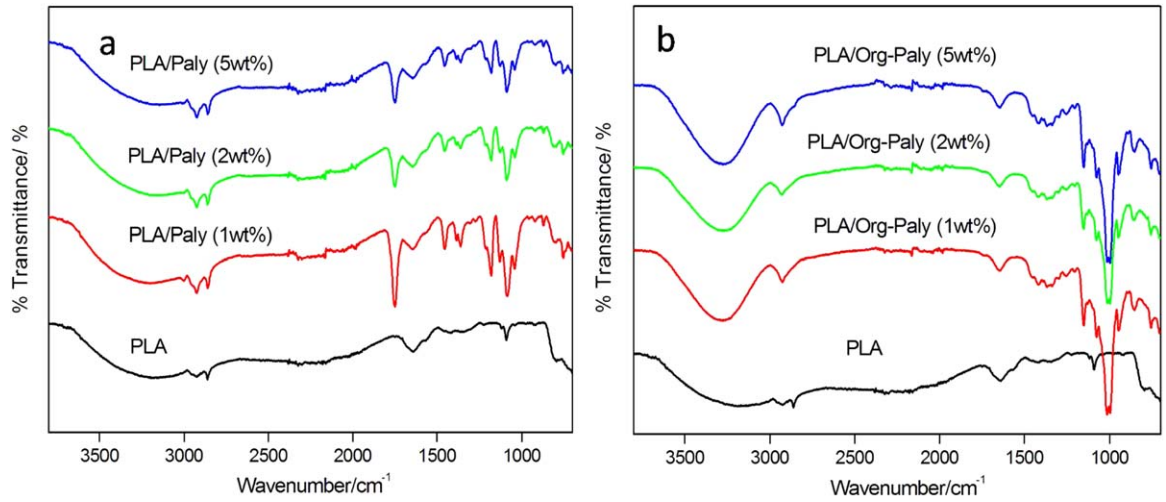

Figure 9. FTIR spectra of (a) PLA and PLA/Paly composites (b) PLA and PLA/Org-Paly composites. [Color figure can be viewed in the online issue, which is available at wileyonlinelibrary.com.]

surface. Raw Paly showed better nucleation effect in comparison to organically modified counterpart as a result of improved dispersion. Incorporation of 2 wt % Paly nanoparticles significantly increased T_g of PLA due to homogeneous dispersion. Though FTIR results showed chemical interaction between organically modified Paly and PLA matrix, higher degree of aggregation had a detrimental effect on the thermal and crystallization properties of these composites.

ACKNOWLEDGMENTS

The authors thank the Department of Science and Technology (DST) and the Council for Scientific and Industrial Research (CSIR), South Africa, for the financial support. Chris Van der Westhuyzen (Biosciences, CSIR, Pretoria) is acknowledged for ^{1}H NMR analyses.

REFERENCES

1. Ikada, Y.; Tsuji, H. *Macromol. Rapid Commun.* **2000**, *21*, 117.
2. Martin, O.; Averous, L. *Polymer* **2001**, *42*, 6209.
3. Yasuniwa, M.; Tsubakihasra, S.; Iura, K.; Ono, Y.; Takahashi, K. *Polymer* **2006**, *47*, 7554.
4. Zhai, W.; Ko, Y.; Zhu, W.; Wong A.; Park, C. B. *Int. J. Mol. Sci.* **2009**, *10*, 5381.
5. Wootthikanokkhan, J.; Cheachun, T.; Sombatsompop, N.; Thumsorn, S.; Kaabbuathong, N.; Wongta, N.; Wong-On, J.; Isarankura Na Ayutthaya, S.; Kositchaiyong, A. J. *Appl. Polym. Sci.* **2013**, *129*, 215.
6. Pavlidou, S.; Papaspyrides, C. D. *Prog. Polym. Sci.* **2008**, *33*, 1119.
7. Lebaron, P. C.; Wang, Z.; Pinnavia, T. J. *Appl. Clay Sci.* **1999**, *15*, 11.
8. Krikorian, V.; Pochan, D. J. *Chem. Mater.* **2003**, *15*, 4317.
9. Wu, T.; Chiang, M. F. *Polym. Eng. Sci.* **2005**, *45*, 1615.
10. Paul, M. A.; Alexandre, M.; Degèe, P.; Henrist, C.; Rulmont, A.; Dubois P. *Polymer* **2003**, *44*, 443.
11. Pluta, M.; Galeski, A.; Alexandre, M.; Paul, M. A.; Dubois, P. *J. Appl. Polym. Sci.* **2002**, *86*, 1497.
12. Nam, P. H.; Fujimori, A.; Masuko, T. *J. Appl. Polym. Sci.* **2004**, *93*, 2711.
13. Di, Y.; Iannace, S.; Di Maio, E.; Nicolais, L. *J. Polym. Sci. B Polym. Phys.* **2005**, *43*, 689.
14. Pluta, M. *Polymer* **2004**, *45*, 8239.
15. Paul, M. A.; Alexandre, M.; Degèe, P.; Calberg, C.; JèrÓme, R.; Dubois, P. *Macromol. Rapid Commun.* **2003**, *24*, 561.
16. Sinha Ray, S.; Maiti, P.; Okamoto, M.; Yamada K.; Ueda, K. *Macromolecules* **2002**, *35*, 3104.
17. Sinha Ray, S.; Yamada, K.; Okamoto, M.; Ueda, K. *Nano Lett.* **2002**, *2*, 1093.
18. Nam, J. Y.; Sinha Ray, S.; Okamoto, M. *Macromolecules* **2003**, *36*, 7126.
19. Lee, J. H.; Jeong, Y. G. *Fiber Polym.* **2011**, *12*, 180.
20. Mclauchlin, A. R.; Thomas, N. L. *Polym. Degrad. Stabil.* **2009**, *94*, 868.
21. Bradley, W. F. *Am. Miner.* **1940**, *24*, 405.
22. Yin, H.; Chen, H.; Chen, D. *Colloids Surf. A Physicochem. Eng. Aspects* **2010**, *367*, 52.
23. Sun, L.; Yang, Z.; Li, X. *Compos. A* **2009**, *40*, 1785.
24. Shen, L.; Lin, Y.; Du, Q.; Zhong, W. *Compos. Sci. Technol.*, **2006**, *66*, 2242.
25. Peng, L.; Zhou, L.; Li, Y.; Pan, F.; Zhang, S. *Compos. Sci. Tech.* **2011**, *71*, 1280.
26. Chen, C. *J. Phys. Chem. Solid.* **2008**, *69*, 1411.
27. Damonte, M.; Torres Snchez, R. M.; dos Santos Afonso, M. *Appl. Clay Sci.* **2007**, *36*, 86.
28. Bakhti, Z. D. A.; Iddou, A.; Larid, M. *Eur. J. Soil Sci.* **2001**, *52*, 683.
29. Kloprogge, T.; Mahmutagic, E.; Frost, R. L. *J. Colloid Interface Sci.* **2006**, *296*, 640.

30. Sarkar, Y. X. B.; Megharaj, M.; Krishnamurti, G. S. R.; Rajarathnam, D.; Naidu, R. *J. Hazard. Mater.* **2010**, *183*, 87.
31. Liu, M.; Pu, M.; Ma, H. *Compos. Sci. Tech.* **2012**, *72*, 1508.
32. Christ, C. L.; Hathaway, J. C.; Hostetler, P. B.; Shepard, A. O. *Am. Miner.* **1969**, *54*, 198.
33. Sabah, E.; Saglam, H.; Kara, M.; Celik, M. S. In Proceedings of Fifth Southern Hemisphere Meeting on Mineral Technology, Argentina, **1996**, p 277.
34. LemicÇ, J.; TomaševicÇ-C anovicÇ, M.; DjuričicÇ, M.; Stanic, T. *J. Colloid Interface Sci.* **2005**, *292*, 11.
35. Fukushima, K.; Tabuani, D.; Camino, G. *Mater. Sci. Eng. C* **2012**, *32*, 1790.
36. Yasuniwa, M.; Sakamo, K.; Ono, Y.; Kawahara, W. *Polymer* **2008**, *49*, 1943.
37. Zhou, H.; Green, T. B.; Joo, Y. L. *Polymer* **2006**, *47*, 7497.
38. Yasuniwa, M.; Tsubakihara, S.; Iura, K.; Ono, Y.; Dan, Y.; Takahashi, K. *Polymer* **2006**, *47*, 7554.
39. Schmidt, S. C.; Hillmyer, M. A. *J. Polym. Sci. B Polym. Phys.* **2001**, *39*, 300.
40. Sabzi, M.; Jiang, L.; Atai, M.; Ghasemi, I. *J. Appl. Polym. Sci.* **2013**.
41. Buzarovska, A.; Grozdanov, A. *J. Appl. Polym. Sci.* **2011**, *123*, 2187.
42. Ash, B. J.; Rogers, D. F.; Wiegand, C. J.; Schadler, L. S.; Siegel, R. W.; Benicewicz, B. C.; Apple, T. *Polym. Compos.* **2002**, *23*, 1014.
43. Jalalvandi, E.; Majid, R. Abd.; Ghanbari, T. *WASET* **2012**, *72*, 773.
44. Kricheldorf, H. R.; Hachmann-Thiessen, H.; Schwarz G. *Biomacromolecules* **2004**, *5*, 492.
45. Sobczak, M. *Polym. Bull.* **2012**, *68*, 2219.
46. Su, Z.; Liu, Y.; Guo, W.; Li, O.; Wu, C. *J. Macromol. Sci. B Phys.* **2009**, *48*, 670.
47. Brizzolara, D.; Cantow, H. J.; Diederichs, K.; Keller, E.; Domb, A. J. *Macromolecules* **1996**, *29*, 191.
48. Cheng, H.; Yang, J.; Frost, R. L.; Wu, Z. *Spectrochim Acta A Mol. Biomol. Spectrosc.* **2011**, *83*, 518.
49. Fukushima, K.; Tabuani, D.; Abbate, C.; Arena, M.; Ferreri, L. *Polym. Degrad. Stabil.* **2010**, *95*, 2049.